RAPID COMMUNICATIONS

PHYSICAL REVIEW B VOLUME 47, NUMBER 15 15 APRIL 1993-I

Time-of-flight measurements of negative differential velocity and electron heating in GaAs/AlAs superlattices

C. Minot, H. Le Person, and J. F. Palmier
FRANCE TELECOM, Centre National d'Etudes des Télécommunications, Laboratoire de Bagneux, 196 avenue Henri Ravera, Boîte Postale 107, 92225 Bagneux CEDEX, France

F. Mollot
Centre National de la Recherche Scientifique, Laboratoire de Microélectronique et de Microstructures, 196 avenue Henri Ravera, Boîte Postale 107, 92225 Bagneux CEDEX, France

(Received 21 December 1992)

We report time-resolved photocurrent measurements of electron time of flight in GaAs/AlAs superlattices. The electron velocity is determined as a function of electric field at 77 and 300 K in a series of superlattices having miniband widths between 22 and 114 meV. Negative differential velocity is evidenced at intermediate electric fields on a picosecond time scale. A Boltzmann-Bloch transport mechanism of the Esaki-Tsu-type is shown to account for the velocity laws when carrier heating is assumed to take place.

Negative differential conductivity has been associated from the beginning with the very idea of superlattice (SL) in semiconductors.[1] Bloch transport has been shown to account for the low-field electron mobilities perpendicular to the layers in $GaAs/Al_xGa_{1-x}As$ (Refs. 2 and 3) and GaAs/AlAs (Ref. 4) SL's having wide minibands ($\Delta > 10$ meV). The alternative mechanism of hopping transport[5,6] is not in agreement with these experiments. In narrow minibands, negative differential conductance (NDC) and photoconductance have been attributed to high-field domain formation,[7,8] Wannier-Stark localization,[9] or miniband conduction.[10] A clear evidence of electron negative differential velocity (NDV) has been obtained in wide miniband GaAs/AlAs (Refs. 11 and 12) SL's. It has been interpreted as originating from the miniband nonparabolicity,[13] in agreement with the Esaki-Tsu model,[1] whereas hopping transport has been shown to disagree with the data. NDC has also been demonstrated in $Ga_xIn_{1-x}As/Al_yIn_{1-y}As$ SL's.[14] Tsu and Esaki have discussed these results in the context of Stark quantization.[15] Recently optical experiments have evidenced the Bloch oscillations,[16] which is a strong support to the Bloch transport model.

NDV is very fast in principle since it relies upon the existence of a miniband structure ($\hbar/\Delta < 66$ fs for $\Delta > 10$ meV) and short momentum relaxation times. Its response time has to be measured in the dynamic regime in order to dismiss any ambiguity about its origin and ascertain its ultimate speed. In this paper we report time-resolved measurements of NDV in wide miniband SL's. The photocurrent impulse response of *n-i-n*-type GaAs/AlAs SL structures is shown to yield the electron time of flight (TOF) in the SL. An optoelectrical TOF technique relying upon the existence of NDV is thus demonstrated on a picosecond time scale at 300 and 77 K. The electron velocity laws which are extracted from the data are compared with the results of several possible transport models.

The samples are grown by molecular-beam epitaxy on GaAs semi-insulating substrates. They consist of an undoped GaAs/AlAs SL (~ 1.4 μm) sandwiched between n^+-type (2×10^{18} cm^{-3}) contact layers (Fig. 1). The top contact layer includes a short-period SL quasialloy acting as a large-gap window layer. Graded composition SL's are grown between layers of different average composi-

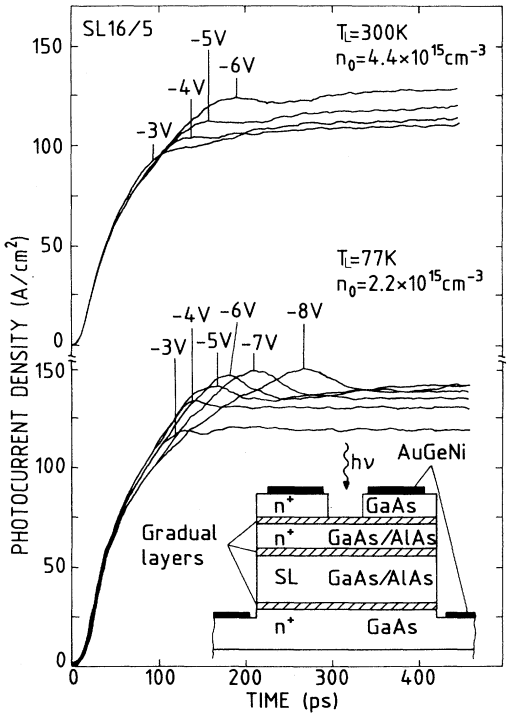

FIG. 1. Photocurrent responses of the 16/5 SL ($\Delta = 30$ meV) as a function of applied voltage at 77 and 300 K. n_0 is the maximum photoexcited carrier density at $t = 0$.

tion to smooth out all conduction-band discontinuities. Small area (3400 μm^2) mesas are processed using conventional photolithographic and etching techniques. The samples are mounted in a cryostat on a 50-Ω microstrip transmission line, which is connected to a 40-GHz sampling oscilloscope through wide band (40 GHz) passive components. The SL is photoexcited by picosecond light pulses ($\sim$3 ps) tunable between 1.675 and 1.82 eV. The time-resolution is limited by the sample capacitance and risetimes as short as 18 ps have been recorded. A series of six SL's is studied here at 77 K, three of them at 300 K. Their miniband widths range from 22 to 114 meV when calculated in the envelope-function scheme using the Kane dispersion relations.[17] In the following they are referred to by the number of atomic monolayers (2.825 Å) in the wells and in the barriers (for instance 16/5).

Figure 1 shows typical photoresponses corresponding to a 16/5 SL ($\Delta=30$ meV) at $T_L=77$ and 300 K, under negative bias on the top contact. The wavelength is adjusted so that the photon energy is slightly above the SL band gap. Only $n=1$ electrons are created (the $n=2$ electron miniband is at least 200 meV above the $n=1$ miniband in all the samples). The photoexcited carrier density is larger than the SL p^- residual doping (5×10^{14} cm^{-3}). At 77 K a distinct photocurrent overshoot is observed at the outset, superimposed over a stronger injection current step. Above -3 V, *the overshoot is increasingly delayed as bias is increased.* Although it is less clear at room temperature, it is still quite observable. This effect is present in all the SL's at 77 and 300 K except in sample 12/4 ($\Delta=78$ meV) at 300 K. It is an evidence of NDV in the time domain, displaying the longer and longer time for photocreated primary electrons to drift throughout the SL as the internal field is increased.

The above interpretation is supported by a time-dependent numerical simulation, based on the one-dimensional classical drift-diffusion equations and Poisson's equation (Fig. 2). They are solved in a finite-difference scheme for a n^+-(GaAs)–p^--(SL)–n^+-(GaAs) three-layered structure with fixed voltage boundary conditions, according to the Scharfetter-Gummel method.[18] The SL is considered as an anisotropic effective medium in which the carrier velocities depend on the local electric field F. The electron velocity law $v(F)=\mu F/(1+|F/F_c|^\eta)$ has three parameters: a low-field mobility μ, a critical field F_c, and an exponent η characterizing the sharpness of NDV for $\eta>1$. This phenomenological relation, which amounts to an Esaki-Tsu law for $\eta=2$ and $\mu F_c=\Delta d/2\hbar$ (d is the SL period), is expected to correctly describe NDV around the critical field. In addition its high-field behavior $F^{1-\eta}$ agrees with the experimental responses for $\eta>1$ since the delay of the overshoot continuously increases with bias.

The temporal evolution of the electron density after photoexcitation by a δ pulse is depicted in Fig. 2(a) for a 16/5 SL at -7 V. The photocreated electrons drift from the cathode to the anode, so that the hole positive charge has to be compensated by additional electrons injected at the cathode. The velocity of holes being very small, their direct contribution to the current is negligible. An electron accumulation builds up thanks to NDV, because the electrons coming from the cathode catch up with the slower electrons near the anode where the field is higher. The overshoot is associated in time with the transit of the electron bump [Fig. 2(b)] and reflects its TOF. As it is absent in the simulated responses when $\eta\leq1$, it can be considered as a signature of NDV.[12,19] It has to be noted that the photoexcited electron density is not large enough

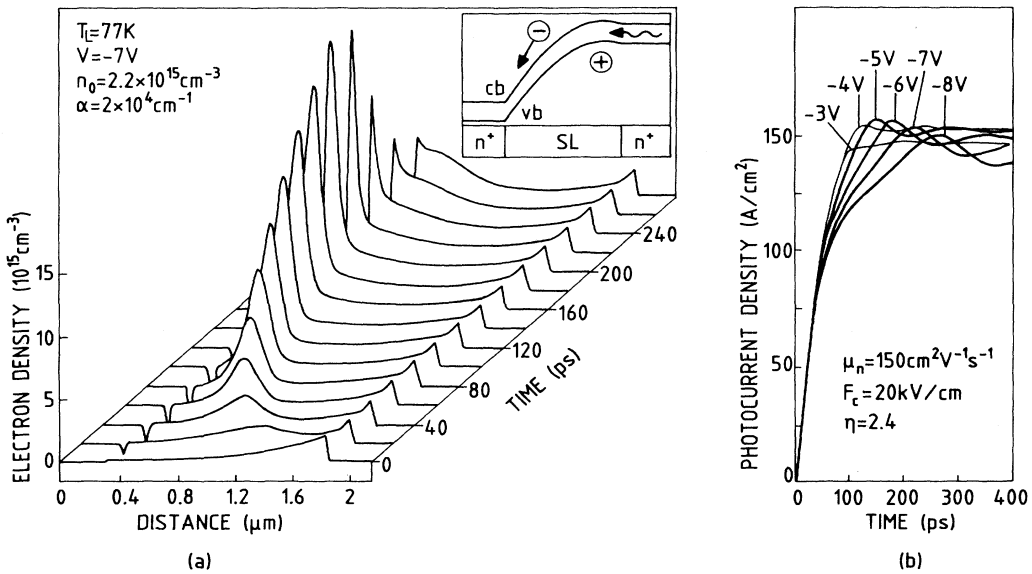

FIG. 2. Simulation results at 77 K for sample 16/5. (a) Time evolution of the electron density distribution at -7 V. $\alpha=2\times10^4$ cm^{-1} is the absorption coefficient. (b) Time evolution of the photocurrent density as a function of applied voltage. The inset shows the band diagram and the motion of the photocreated carriers.

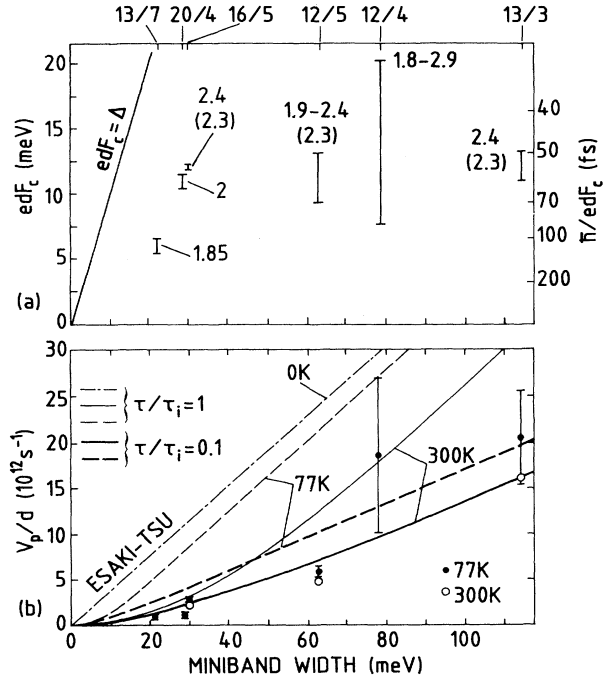

FIG. 3. (a) Potential drop over one period at the critical field vs miniband width. There is no difference between $T_L=77$ and 300 K within experimental error. η is also given at 77 and 300 K in parentheses. (b) Experimental [(●), $T_L=77$ K; (○), $T_L=300$ K] and calculated [(– – –), $T_L=77$ K, (——), $T_L=300$ K] variations of v_p/d (peak velocity over SL period) vs miniband width, for $\tau/\tau_i=1$ (thin lines) and $\tau/\tau_i=0.1$ (thick lines). The error bars correspond to the range of allowed values in the fitting procedure described in the text.

to alter the band diagram significantly, in contrast to recent results obtained at higher excitation intensity.[20]

The numerical simulation makes it possible to fit the experimental responses accurately [Figs. 1 and 2(b)] by adjusting μ, F_c, and η in order to obtain the correct variations of the delay between the onset of the photoresponse and the maximum of the overshoot at different applied voltages and, to a lesser degree, the correct current amplitudes. As the fit is primarily sensitive to the product μF_c, i.e., the peak velocity, responses under positive bias are also used to reduce the uncertainty on F_c. The results are summarized in Fig. 3 in terms of η, edF_c the potential drop over one period at the critical field [Fig. 3(a)], and v_p/d the peak velocity over the period [Fig. 3(b)]. In the Esaki-Tsu model, edF_c and v_p/d are proportional to the inverse momentum relaxation time ($edF_c=\hbar/\tau$) and to the miniband width ($v_p/d=\mu F_c/2d=\Delta/4\hbar$), respectively.

Intervalley transfer is responsible for NDV in bulk III-V materials. It has been rejected as a dominant mechanism in SL's,[13] because current-voltage and pressure-dependent measurements are insensitive to the Γ-X and Γ-L separation energies. This is in agreement with our data for the critical fields F_c (or edF_c) are uncorrelated with the energy separation between X or L levels and the top or the bottom of the Γ_1 miniband.

Two other mechanisms have been invoked to explain the microscopic origin of NDV: (i) the negative effective mass effect,[1] (ii) the Wannier-Stark localization.[2] In principle, (i) and (ii) are physically equivalent.[19] They lead to different results because they rest upon different transport equations, which are not reducible to each other:[21] (i) rests upon Boltzmann-Bloch transport and (ii) upon hopping transport. Hopping is not in agreement with the present data for the experimental velocity is markedly larger than theoretically predicted[6] (by about two orders of magnitude in sample 16/5 at room temperature for a field $F=\Delta/ed$), and it is a decreasing function of temperature between 77 and 300 K. On the other hand, our results can be quantitatively explained by a simple one-band model, exactly solving the Boltzmann equation in a constant relaxation time approximation, and taking carrier heating into account. Elastic and inelastic collisions are assumed to additively relax the distribution function with distinct relaxation times τ_e and τ_i, towards a heated and an equilibrium Maxwellian, respectively. The overall momentum relaxation time is $\tau=\tau_i\tau_e/(\tau_i+\tau_e)$, and τ_i is the energy relaxation time. The field-dependent electron temperature T_E obeys an energy balance equation in which elastic collisions do not dissipate the total (in-plane and miniband) energy. The velocity is then given by

$$v(F)=\left[1+\frac{\tau}{\tau_e}(2k_BT_E/\Delta-2k_BT_L/\Delta)\times\frac{I_0(\Delta/2k_BT_L)}{I_1(\Delta/2k_BT_L)}\right]\frac{\mu F}{(1+|F/F_0|^2)},$$

where I_0 and I_1 are Bessel functions. The mobility is $\mu=(e\tau/M)I_1/I_0$ with $M^{-1}=\Delta d^2/2\hbar^2$, and $F_0=\hbar/ed\sqrt{\tau\tau_i}$. The peak velocity is governed by the miniband width and the ratio τ/τ_i. It is approximately reduced by a factor $\sqrt{\tau/\tau_i}$ with respect to the Esaki-Tsu result, which is recovered when $\tau=\tau_i$ and $T_L=0$. Only the critical field depends on the magnitude of τ and τ_i. It is intermediate between $\hbar/ed\sqrt{\tau\tau_i}$ and $\hbar/ed\tau$.

The experimental peak velocities are in agreement with $\tau/\tau_i=0.1$ [Fig. 3(b)]. The critical field then yields the relaxation times $\tau\sim30$–45 fs and $\tau_i\sim300$–450 fs [Fig. 3(a)]. Energy relaxation thus occurs on a much longer time scale than momentum relaxation. As a result, the electrons are significantly heated by the field. The model gives the electron temperature at the critical field: $T_E=420$, 580, and 780 K for $\Delta=30$, 63, and 114 meV, respectively, at room temperature. This is consistent with more detailed time-dependent calculations in which accurate collision integrals have been used. Strong elastic scattering has to be invoked to account for fast momentum relaxation. We believe that interface roughness contributes dominantly.[22] Carrier-carrier collisions should also be considered because they alter the average velocity due to the nonparabolic miniband dispersion. At $T_L=77$ K, $\tau/\tau_i\sim0.1$ is too large for the narrowest minibands [Fig. 3(b)]. Smaller values would lead to very long energy relaxation times, and it is likely that a more complex transport mechanism involving localization takes place in those SL's.

In conclusion, time-resolved photocurrent measurements in GaAs/AlAs SL's yield the variations of the electron TOF in the SL and give evidence of electron NDV. It is shown that NDV obeys Boltzmann-Bloch transport and can be a fast process, although carrier heating by the field, resulting from different momentum and energy relaxation times, reduces the maximum stationary drift velocities.

The authors wish to thank J. C. Esnault and S. Vuye for their assistance in the technological processing of the samples and Dr. H. Grahn for a fruitful discussion.

[1]L. Esaki and R. Tsu, IBM J. Res. Dev. **14**, 61 (1970).
[2]J. F. Palmier, C. Minot, J. L. Lievin, F. Alexandre, J. C. Harmand, J. Dangla, C. Dubon-Chevallier, and D. Ankri, Appl. Phys. Lett. **49**, 1260 (1986).
[3]B. Deveaud, J. Shah, T. C. Damen, B. Lambert, and A. Regreny, Phys. Rev. Lett. **58**, 2582 (1987).
[4]C. Minot, H. Le Person, J. F. Palmier, and R. Planel, Superlatt. Microstruct. **6**, 309 (1989).
[5]R. Tsu and G. Döhler, Phys. Rev. B **12**, 680 (1975).
[6]D. Calecki, J. F. Palmier, and A. Chomette, J. Phys. C **17**, 5017 (1984).
[7]L. Esaki and L. L. Chang, Phys. Rev. Lett. **33**, 495 (1974).
[8]K. K. Choi, B. F. Levine, R. J. Malik, J. Walker, and C. G. Bethea, Phys. Rev. B **35**, 4172 (1987).
[9]R. Tsu, L. L. Chang, G. A. Sai-Halasz, and L. Esaki, Phys. Rev. Lett. **34**, 1509 (1975).
[10]H. T. Grahn, K. von Klitzing, K. Ploog, and G. H. Döhler, Phys. Rev. B **43**, 12 094 (1991).
[11]A. Sibille, J. F. Palmier, C. Minot, and F. Mollot, Appl. Phys. Lett. **54**, 165 (1989).
[12]H. Le Person, J. F. Palmier, C. Minot, J. C. Esnault, and F. Mollot, Surf. Sci. **228**, 441 (1990).
[13]A. Sibille, J. F. Palmier, H. Wang, and F. Mollot, Phys. Rev. Lett. **64**, 52 (1990).
[14]F. Beltram, F. Capasso, D. L. Sivco, A. L. Hutchinson, S. N. G. Chu, and A. Y. Cho, Phys. Rev. Lett. **64**, 3167 (1990).
[15]R. Tsu and L. Esaki, Phys. Rev. B **43**, 5204 (1991).
[16]J. Feldmann, K. Leo, J. Shah, D. A. B. Miller, J. E. Cunningham, T. Meier, G. von Plessen, A. Schulze, P. Thomas, and S. Schmitt-Rink, Phys. Rev. B **46**, 7252 (1992).
[17]G. Danan, B. Etienne, F. Mollot, R. Planel, A. M. Jean-Louis, F. Alexandre, B. Jusserand, G. Le Roux, J. Y. Marzin, H. Savary, and B. Sermage, Phys. Rev. B **35**, 6207 (1987).
[18]D. L. Scharfetter and H. K. Gummel, IEEE Trans. Electron Devices **ED-16**, 64 (1969).
[19]C. Minot, H. Le Person, F. Mollot, and J. F. Palmier, Proc. SPIE **1362**, 301 (1991).
[20]H. Le Person, C. Minot, L. Boni, J. F. Palmier, and F. Mollot, Appl. Phys. Lett. **60**, 2397 (1992).
[21]J. R. Barker, *Handbook on Semiconductors* (North-Holland, Amsterdam, 1982), Vol. I, p. 617.
[22]J. F. Palmier, G. Etemadi, A. Sibille, M. Hadjazi, F. Mollot, and R. Planel, Surf. Sci. **267**, 574 (1992).